Design of a Test Rig for Two-Phase Turbo-expander Characterization

Simone Parisi[a,], Roberto Agromayor[a], Nishith B. Desai[a] and Fredrik Haglind[a]*

[a] *Technical University of Denmark, Kongens Lyngby, Denmark,*
[*] *Corresponding Author, sipar@dtu.dk*

Abstract:
The expansion of two-phase mixtures offers significant efficiency gains in partial-evaporation organic Rankine cycles (ORC) and refrigeration systems. However, the development of high-efficiency two-phase turboexpanders remains hindered by a lack of high-fidelity experimental data and validated design models. To address this gap, this paper presents the comprehensive design of a 100 kW-thermal laboratory-scale test facility dedicated to the characterization of two-phase turboexpanders. A novel measurement strategy utilizing an isenthalpic throttling valve is introduced to precisely determine the turbine inlet vapor quality, thereby circumventing the high uncertainties associated with traditional energy-balance methods. Furthermore, a rigorous fluid screening and thermodynamic scaling analysis identifies Novec 649 as the optimal working fluid, thanks to its excellent safety profile and favorable physical properties that enable the investigation of both two-phase and wet-to-dry expansion regimes. Finally, a parametric analysis maps the operating envelope to define component sizing requirements. The proposed facility will generate the high-quality datasets necessary to validate multiphase computational models and establish robust design guidelines for future two-phase turbomachinery.

Keywords:
Two phase Turbine, Partial Evaporation ORC, Test Rig.

1 Introduction

The expansion of two-phase mixtures offers great potential to improve energy conversion efficiency across a range of applications. In power generation, trilateral and partial-evaporation organic Rankine cycle (ORC) systems can achieve better temperature matching with sensible heat sources, enabling higher heat source utilization and up to 80 % more net power output compared to conventional ORC systems [1]. This capability could transform previously uneconomical low-temperature heat sources, such as geothermal brines and industrial waste heat streams, into viable targets for power generation [2]. Similarly, in refrigeration and heat pump systems, replacing Joule-Thomson expansion valves with two-phase expanders reduces the irreversibility of the throttling process by recovering part of the expansion work. This not only offsets the compression work, but also increases the liquid fraction at the evaporator inlet and the associated cooling capacity, improving the coefficient of performance (COP) by up to 50 % depending on the working fluid and operating conditions [3].
While these system-level benefits are significant, they can only be realized if the two-phase expander achieves sufficiently high isentropic efficiency. For example, an analysis of partial-evaporation ORC systems for low-temperature geothermal heat sources shows that the system-level advantages are eliminated when the isentropic efficiency of the two-phase expander is reduced by more than 20 % relative to that of a single-phase machine [4]. In refrigeration and heat pump systems, two-phase expanders must outperform the COP of system employing ejectors to be competitive. In one case Ersoy et al. [5] found that the two-phase expander must achieve isentropic efficiencies above approximately 70 % to be competitive. The central question is therefore not whether two-phase expansion is

thermodynamically beneficial, but whether it is possible to design expanders that achieve the required efficiency levels and operate reliably under two-phase flow conditions.

Two main classes of two-phase expanders exist: volumetric machines and turboexpanders. Volumetric machines are attractive for two-phase expansion due to their flexible operating range, inherent tolerance to gas-liquid flows without erosion, and the possibility of retrofitting existing compressor hardware from refrigeration systems to operate in reverse as an expander [6]. Among volumetric machines, twin-screw expanders have been the primary focus of development. Smith et al. [7] tested prototypes with built-in volume ratios from 3 to 9 and achieved peak isentropic efficiencies exceeding 70 % under two-phase conditions. More recently, Dawo et al. [8, 9] operated a commercial twin-screw compressor as an expander in a partial-evaporation ORC system, reporting combined electrical isentropic efficiencies of up to 50 % and system-level exergy efficiency gains of up to 80 % over single-phase ORC operation. While these results confirm the feasibility of volumetric expanders, this technology faces several limitations. They typically rely on oil lubrication to reduce internal leakage, which can contaminate the working fluid and degrade system performance [10]. Moreover, their size and cost scale rapidly with power output, making them less attractive for medium-to-large scale applications [11]. Finally, their built-in volume ratio is fixed by geometry and typically remains below 10, limiting the expansion achievable within a single machine [11].

Turboexpanders present a compelling alternative to address these limitations. They require no lubrication oil, and their power output scales favorably with the cube of blade speed, enabling more compact machines at large power outputs. Additionally, they can accommodate larger volumetric expansion ratios within a single machine, either by stacking multiple stages in series or by using converging-diverging blading that accelerates the fluid to supersonic speeds. Despite these advantages, two main concerns have historically been raised against two-phase turboexpanders: the risk of blade erosion from droplet impacts, and low isentropic efficiencies [2, 12].

Erosion is a well-established risk in steam turbines [13], where large enthalpy drops produce high-velocity flows that can exceed the damage threshold of the blade material. By contrast, working fluids used in two-phase turbines for ORC and refrigeration systems have significantly higher molecular mass than water, resulting in lower enthalpy drops and jet velocities for the same expansion ratio, making erosion damage less likely. Welch & Boyle [14] confirmed this experimentally with a two-phase axial impulse turbine for a partial-evaporation ORC system, reporting maximum droplet impact velocities in the range from 90 $\mathrm{m/s}$ to 150 $\mathrm{m/s}$, well below the erosion threshold of the titanium alloy rotor, which exceeds 300 $\mathrm{m/s}$. No signs of erosion were observed after 150 hours of two-phase operation. Hays et al. [15] replicated these findings over a longer operation period, demonstrating a partial-evaporation ORC waste heat recovery unit that accumulated over 4,000 hours of marine service with no blade erosion observed after teardown inspection.

Regarding efficiency, and as surveyed in Kumar et al. [16], the isentropic efficiency of two-phase turbines has improved steadily from around 23 % in early prototypes to above 70 % in the most advanced designs, confirming that efficiencies comparable to twin-screw expanders are achievable. Despite this progress, their development has largely relied on iterative trial-and-error rather than on established design guidelines and systematic optimisation [16]. Moreover, the lack of high-quality experimental datasets has hindered the development and validation of numerical models required to guide the design of high-efficiency two-phase turboexpanders, suggesting that further efficiency gains are possible.

Recognizing this lack of experimental data, Lhermet et al. [17] conducted the only published experimental study of a two-phase axial turbine in a partial-evaporation ORC system. A commercial single-phase impulse turbine was operated under two-phase inlet conditions, demonstrating stable operation and a relatively modest efficiency penalty of about 4 percentage points as the liquid mass fraction increased from 0 % to 35 %. While these results are encouraging, the dataset remains insufficient to support the validation of two-phase flow models. First, the study is limited to a single, undisclosed turbine geometry and performance tested at a single rotational speed. Second, the tur-

bine inlet thermodynamic state was not measured directly but inferred from an energy balance on the evaporator, resulting in an uncertainty of approximately ±10 % in the inlet vapor quality. Finally, the reported peak isentropic efficiency is only 27 %, which the authors attribute to the small scale of the machine and the use of partial admission. However, the instrumentation used and data reported do not allow these losses to be distinguished from those due to two-phase flow phenomena such as non-equilibrium phase change in the nozzle or liquid segregation within the rotor.

Overall, the lack of high-quality experimental datasets across different geometries and operating conditions remains a key barrier towards the validation of predictive models and the development of design guidelines for two-phase turboexpanders. To address this gap, this paper presents the design of a laboratory-scale test facility for the experimental characterization of two-phase turboexpanders. Although the facility operates as a partial-evaporation ORC unit, its system layout and instrumentation are designed to accurately characterize two-phase turbine performance, with findings applicable to other application areas such as refrigeration and heat pump systems. A dedicated measurement strategy employing an isenthalpic throttling valve is introduced to determine the turbine inlet state, reducing the uncertainty in inlet vapor quality relative to energy-balance approaches used in prior experimental studies. A fluid screening is conducted to identify a suitable working fluid based on thermodynamic performance, environmental impact, and safety considerations. In addition, a sensitivity analysis is performed to assess the influence of turbine inlet temperature and vapor quality on the required thermal power and the isentropic Mach number in the turbine. This facility will provide high-quality experimental data to the validation of numerical models as well as the development of new design guidelines for two-phase turboexpanders.

The remainder of the paper is organized as follows. Section 2 describes the configuration of the test rig, including the system layout and the new strategy to measure the turbine inlet conditions. Section 3 presents the thermodynamic model used for fluid screening and test rig sizing. Section 4 discusses the results of the fluid screening and the analysis of the test rig operating envelope. Finally, Section 5 summarizes the main findings and outlines directions for future work.

2 Test rig configuration

A typical ORC consists of four basic components: a pump, a heater, a turbine, and a condenser. The most critical component for the safe operation of an ORC test rig is the pump, as insufficient subcooling can cause cavitation and severe damage. Section 2.1 describes different configurations considered to ensure pump subcooling. Furthermore, accurately characterizing the turbine inlet state is challenging: because it lies in the two-phase region, pressure and temperature are coupled and cannot uniquely define the thermodynamic state. Section 2.2 presents different strategies considered to solve this problem.

2.1 Control of pump subcooling

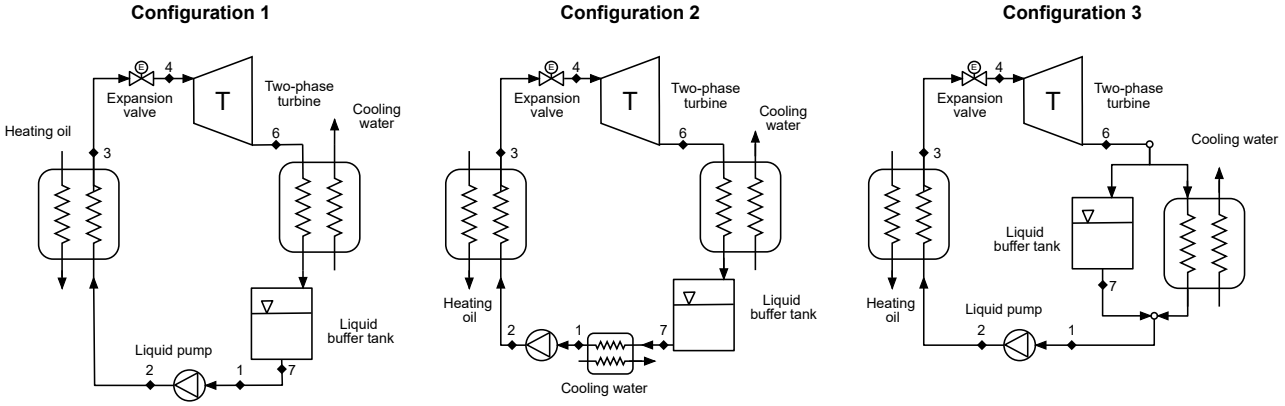

Figure 1: Comparison of various condenser and liquid receiver configurations.

Figure 1 illustrates three different configurations investigated for the condenser and liquid buffer (receiver) tank, differing in their layout and placement. For all configurations, the corresponding state points are labeled 1 through 7. A plate heat exchanger and a separate liquid receiver were preferred as a more compact solution compared to a flooded shell-and-tube design. Consequently, alternative strategies to induce subcooling, such as introducing non-condensable gases into the condenser [18], were deemed unfeasible.
In configuration 1, subcooling is achieved by placing the pump at a lower elevation. While simple and reliable, this configuration is bulky and unsuitable for a small test rig. Configuration 2 uses a separate heat exchanger to provide subcooling, offering the highest degree of control. Configuration 3 uses a partially flooded heat exchanger acting both as condenser and subcooler. Mixing of the condenser outlet with the saturated liquid in the receiver makes the subcooling less stable during transients. Configuration 2 was ultimately selected due to its compactness and stability during transient operation.

2.2 Measurement of turbine inlet conditions

Since pressure and temperature do not define a thermodynamic state for a pure substance under vapor-liquid equilibrium, several approaches were evaluated to estimate the turbine inlet state.
Solution 1: Heat balance through the main heat exchanger. The heating oil temperatures and mass flow rate are known and can be used to calculate the transferred heat. While requiring no additional equipment, the assumed fraction of ambient heat loss introduces significant uncertainty.
Solution 2: Quality measurement of the two-phase mixture. Direct measurement of mixture quality is exceptionally challenging and requires extensive calibration of specialized equipment, such as wire mesh sensors [19].
Solution 3: Phase separation and flow rate measurement. The quality can be measured by separating the liquid and gas, and measuring independently the mass flow rate of each phase. While accurate, it drastically increases system complexity, footprint, and cost.
Solution 4: Isenthalpic expansion of subcooled liquid. In this solution, heat transfer in the main exchanger occurs entirely in the single-phase region. The fluid then passes through a well-insulated throttling valve, reducing pressure while keeping a constant mixture enthalpy. This enables the determination of the turbine inlet state using only an additional pressure sensor after the valve, while also allowing accurate control of the inlet conditions by adjusting valve opening.
Solution 4 is selected as the most suitable approach for the proposed test rig. While it reduces overall cycle efficiency by requiring higher upstream pressures and temperatures, cycle efficiency is secondary to accurately characterizing two-phase turbine performance under controlled inlet conditions. By contrast, the simpler Solution 1 would be recommended for industrial-scale applications where high efficiency is the primary driver.

3 Thermodynamic model

The thermodynamic model selected for the test rig sizing is based on the assumptions of steady-state operation and thermodynamic equilibrium in each section, using the CoolProp [20] library for the fluid property calculations. The thermodynamic calculations are based on the REFPROP 10 [21] backend, considering the default equation of state for each fluid.
Table 1 summarizes the imposed conditions used to determine each thermodynamic state. The heater power, used as a sizing variable, is based on the availability of hot oil from a 100 kW electric heater. The condenser temperature selected represents a conservative value because an intermediate water loop will be added between the cooling water and refrigerant circuit to guarantee stable cooling conditions. The turbine isentropic efficiency is kept equal to unity in order to obtain an upper estimate of the torque and power it can generate, which will be used for the sizing of the generator and shaft. The turbine inlet (point 4 in Figure 1) is fixed by imposing the quality and the reduced temperature. The test rig sizing is done at the heater's "maximum power point". The maximum power point is

Table 1: Assumptions adopted for the thermodynamic cycle calculations.

Quantity	Symbol	Value	Unit
Common conditions			
Pump inlet subcooling	$\Delta T_{1,\text{subcooling}}$	5	K
Heater outlet subcooling	$\Delta T_{3,\text{subcooling}}$	5	K
Pump isentropic efficiency	$\eta_{\text{is,p}}$	0.7	–
Turbine isentropic efficiency	$\eta_{\text{is,t}}$	1.0	–
Heater pressure loss	$1 - P_3/P_2$	0.03	–
Condenser pressure loss	$1 - P_1/P_7$	0.03	–
Maximum power point			
Turbine inlet vapor quality	x_4	0.05	–
Turbine reduced inlet temperature	T_{4r}	0.95	–
Condensation temperature	T_7	333.15	K
Heater power	$\dot{Q}_{\text{heater}}$	90.0	kW

defined as the point with the highest reduced temperature and lowest inlet quality, as this combination leads to the highest flow rate through the throat of the turbine nozzle. The working fluid state at the heater outlet is computed from the turbine inlet considering an isenthalpic expansion through the valve. The pressure at the inlet of the valve is iteratively computed to satisfy the imposed subcooling, defined as the difference between the saturation temperature T_{sat} at the fluid pressure P_i, and the fluid temperature T_i:

$$\Delta T_{i,\text{subcooling}} = T_{\text{sat}}(P_i) - T_i \tag{1}$$

The pump outlet pressure is calculated from the pressure drop in the heater. The pump inlet state is fully defined from the condenser saturation pressure and the degree of subcooling. The pump outlet state is calculated by applying the definition of isentropic efficiency of the pump:

$$\eta_{\text{is,p}} = \frac{h(P_2, s_1) - h_1}{h_2 - h_1} \tag{2}$$

The turbine outlet is calculated in a similar fashion using the pressure loss in the condenser and the definition of isentropic efficiency of the turbine:

$$\eta_{\text{is,t}} = \frac{h_6 - h_4}{h(P_6, s_4) - h_4} \tag{3}$$

The procedure described up to this point is sufficient to compute all thermodynamic states, but not the mass flow rate. For all pressure ratios of interest, the turbine is expected to be choked. Under this condition, the mass flow rate can be calculated from the sonic conditions at the throat. Because the turbine inlet is already two-phase, negligible metastable effects are expected in the throat, and thermodynamic equilibrium is assumed. The turbine nozzle is assumed to be accelerating the flow in an isentropic way and the effect of slip between the phases is neglected, leading to the following conditions:

$$h_{\text{th}} = h_4 - \frac{1}{2} v_{\text{th}}^2 \quad \text{and} \quad s_{\text{th}} = s_4 \tag{4}$$

where the subscript "th" refers to the nozzle throat. The sonic condition, indicated with the asterisk superscript, is obtained by maximizing the mass flux through the throat:

$$v^* = \underset{v_{\text{th}}}{\text{argmax}} \left(v_{\text{th}} \cdot \rho \left(h_{\text{th}} \left(v_{\text{th}} \right), s_{\text{th}} \right) \right) \tag{5}$$

The mass flow rate $\dot{m}$ and heater power $\dot{Q}_{\text{heater}}$ are then computed respectively as:

$$\dot{m} = v^* \rho^* A_{\text{th}} \tag{6}$$

$$\dot{Q}_{\text{heater}} = \dot{m}\left(h_3 - h_2\right) \tag{7}$$

The nozzle throat area can be obtained by imposing the heater heat flow rate at the maximum power point. Once the throat area is defined, the off-design operation of the test rig can be investigated by keeping the throat area constant and parametrically changing the turbine inlet conditions.
To verify that the turbine is actually choked, the conditions at the nozzle outlet (state point 5) must be evaluated. Under isentropic flow assumptions, a Mach number greater than unity indicates a choked state. Assuming an impulse turbine, the pressure at the nozzle outlet is taken equal to the turbine outlet pressure, and the nozzle outlet enthalpy is obtained from the isentropic expansion:

$$h_5 = h(P_6, s_4) \tag{8}$$

The corresponding flow velocity then follows from the energy balance:

$$v_5 = \sqrt{2\left(h_4 - h_5\right)} \tag{9}$$

and, the Mach number is computed using the local speed of sound:

$$M_5 = \frac{v_5}{a(h_5, s_4)} \tag{10}$$

Finally, the turbine rotational speed ω can be estimated using the definition of specific speed ω_s based on total conditions:

$$\omega = \omega_s \frac{\left(h_4 - h_6\right)^{3/4}}{\left(\dot{m}/\rho_6\right)^{1/2}} \tag{11}$$

where a specific speed of $\omega_s = 0.4$ is selected for this study, as this value is considered the lower boundary for high-efficiency designs [22].

3.1 Droplet size scaling

Given the large power ratings typical for the application of turbomachinery, testing of novel concepts is usually done at reduced scale. However, unlike for single phase flows, scaling laws for two-phase flow testing do not allow to maintain strict dynamic similarity. The droplet size in a nozzle is highly dependent on the geometry and the complex interaction of non-equilibrium, non-constant acceleration, and the evolution of the properties of each phase along the length of the nozzle. In this analysis, simplified assumptions are used to derive a scaling law for droplet size. The purpose of this derivation is to compare the relative effect of fluid choice on droplet size, and is not expected to yield accurate quantitative predictions in absolute terms.
In this simplified model, the acceleration in the converging part of the nozzle is assumed to be uniform, and the liquid is assumed to be accelerated by the gas through aerodynamic drag. The force necessary to accelerate the droplet is:

$$F = \left(\rho_L - \rho_V\right)\left(\frac{\pi}{6} D_P^3\right)\ddot{x} \tag{12}$$

where ρ_L and ρ_V are the saturated liquid and vapor densities, computed at the sonic condition, D_P the particle diameter, and the convective acceleration $\ddot{x}$ can be computed from the convergent section length L and the average mixture velocity at the throat v^* as:

$$\ddot{x} = \frac{v^{*2}}{2L} \tag{13}$$

At equilibrium, the equation for aerodynamic drag is:

$$F = \frac{1}{2}\rho_V \Delta v^2 \left(\frac{\pi}{4} D_P^2\right) C_d \tag{14}$$

where Δv is the equilibrium slip velocity between the phases and the aerodynamic drag coefficient is taken equal to $C_d = 0.4$, corresponding to the laminar separation regime for a sphere, valid for Reynolds numbers between $8 \cdot 10^2$ and $2 \cdot 10^5$ [23]. Because both the slip velocity and droplet diameter are unknown, an additional closure equation is necessary. The definition of Weber number We is used in this case:

$$\mathrm{We} = \frac{\rho_V \Delta v^2 D_P}{\sigma} \tag{15}$$

where σ is the surface tension. The equilibrium Weber number is assumed to be $\mathrm{We} = 12$. This condition is based on experimental evidence [24], and is valid for an Ohnesorge number (On) lower than 0.1:

$$\mathrm{On} = \frac{\mu_L}{\left(\rho_L D_P \sigma\right)^{0.5}} \tag{16}$$

where μ_L is the viscosity of the liquid phase.
The equations above can be rearranged to solve for the droplet diameter as:

$$D_P = \sqrt{\frac{3 C_d \mathrm{We}}{8}} \cdot \sqrt{L} \cdot \sqrt{\frac{\sigma}{\left(\rho_L - \rho_V\right) v^{*2}}} \tag{17}$$

The first term of Eq. 17 is a numerical constant, the second depends on the scale of the turbine, while the last is obtained from thermodynamic quantities that are independent of scale. As the turbine is scaled down, the nozzle convergent length L and the throat diameter D_{th} are reduced by the same factor, however, the droplet diameter decreases more slowly due to the square root. For this reason, as the turbine is scaled down the ratio D_{th}/D_P reduces, or in other words the droplets become relatively bigger compared with the throat diameter. In this work the ratio D_{th}/D_P is estimated based on typical values encountered in turbine design, assuming that the convergent length is equal to twice the throat diameter and that the throat area is distributed between fifteen circular passages. It should be noted that Eq. 17 cannot be used too close to the critical point, since as the surface tension decreases the condition on the Ohnesorge number is not verified.

4 Simulation results

4.1 Fluid screening

One of the characteristics of ORC power systems is the variety of working fluids that can be employed. In addition to compliance with safety and environmental requirements, typical working fluids screenings focus on maximizing cycle performance or minimizing the cost of the produced electricity. Fluid selection for a test setup, however, is governed by a different objective: gaining the most varied and precise amount of scientifically and industrially relevant data within the limitations imposed by available resources and laboratory conditions. In a partial evaporation ORC systems, the turbine is the component which most significantly differs from conventional ORC units, its investigation is therefore of great importance. Given the small scale of the test rig, it is considered important to select a fluid leading to a large throat area. A larger turbine is easier to instrument and rotates at a lower speed, which results in better availability of off the shelf components such as bearings, torque sensors, and generator.
A total of 124 candidate fluids were considered and screened based on the following criteria: (i) the fluid must be a pure substance; (ii) the critical temperature must exceed 373.15 K and the triple-point temperature must be below 273.15 K, ensuring the existence of a liquid phase within the temperature range of interest; (iii) the saturation pressure at 293.15 K must be higher than 20 kPa, in order to avoid operation under extreme vacuum conditions, which would increase sensitivity to non-condensable gases entering the system through small leakages at the turbine shaft seal; and (iv) the Mach number

Table 2: Results of the fluid screening.

fluid	P_{amb} [kPa]	P_3 [kPa]	T_3 [°C]	A_{th} [mm^2]	Ma_5	ω [kRPM]	D_{th}/D_P
Novec649	32.59	1448.27	148.44	75.16	1.79	21.77	301.89
R236FA	229.36	2588.71	107.75	74.73	1.43	22.51	361.04
R142b	288.81	3377.67	119.90	50.82	1.49	34.72	352.81
R1234ze(Z)	148.81	2882.33	132.12	47.61	1.63	35.43	324.33
R245fa	123.06	2947.43	135.42	43.04	1.68	36.37	316.30
IsoButane	302.22	3034.31	117.16	42.89	1.44	51.19	337.74
R1233zd(E)	108.15	2948.71	147.56	41.68	1.75	38.01	319.37
R123	75.61	2983.14	164.08	39.58	1.87	36.28	317.16
R113	36.68	2748.32	192.78	36.76	2.08	34.59	299.38

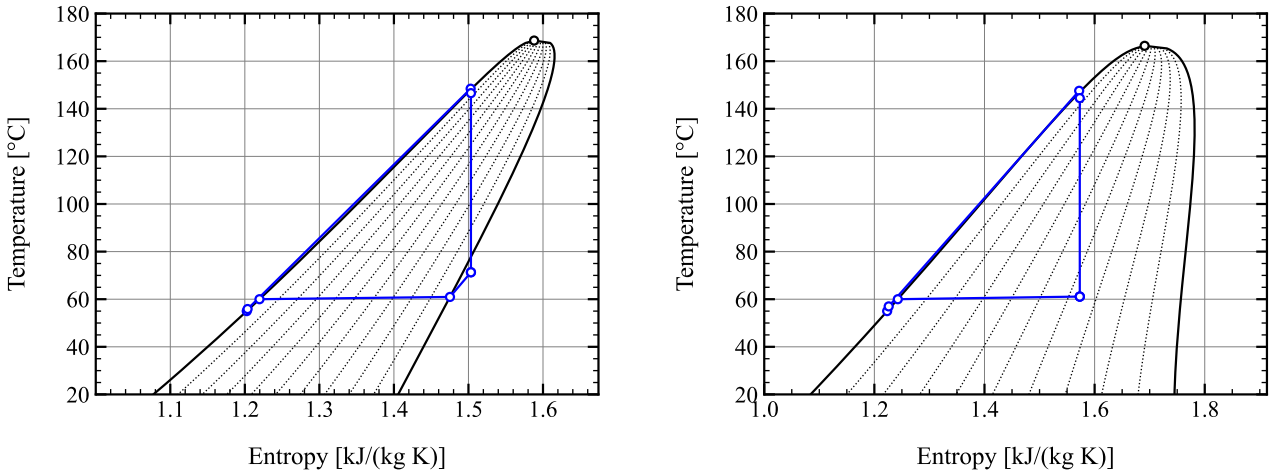

(a) Novec 649

(b) R1233zd(E)

Figure 2: Temperature-entropy diagrams at the maximum power point.

at the nozzle outlet must exceed 1.4, ensuring a supersonic expansion representative of industrial two-phase turbines with converging–diverging stator blades. This latter condition enables the design of such blade geometries using the method of characteristics [25].

Out of the complete list, 27 fluids produced a solution that satisfies the above criteria. Table 2 presents the ten most promising fluids, listed from largest to smallest throat area. Small variations can be observed in the relative droplet size among fluids. Therefore, the effect of droplet size can be generalized to different working fluids. Among the investigated fluids, the two most promising options for a test-rig are Novec 649 and R1233zd(E) as they satisfy these additional requirements: (i) good environmental profile in terms of low global warming potential (GWP < 150) and zero ozone depletion potential (ODP = 0); and (ii) excellent safety profile, belonging to ASHRAE safety class A1 (non-toxic and non-flammable). The non flammability requirement excludes hydrocarbons, which are considered promising options for partial evaporation ORC units [4]. The use of flammable fluids would increase the cost and complexity for indoor installations, while for larger plants the low cost of hydrocarbons is a predominant factor.

Figure 2 presents the temperature-entropy diagram and thermodynamic states for the Novec 649 and R1233zd(E) cycles. Novec 649 is a dry fluid, and at the maximum power point the two phase expansion crosses the vapor saturation line. This condition is known as wet-to-dry expansion, and is also of interest. If the turbine inlet temperature was to be decreased, the expansion could be brought back within the two-phase region. This makes Novec 649 an ideal candidate to investigate a wide variety of flow regimes within a single test rig and fluid. The shape of the vapor saturation line of R1233zd(E), on the other hand, is nearly isentropic, similar to most hydrocarbons.

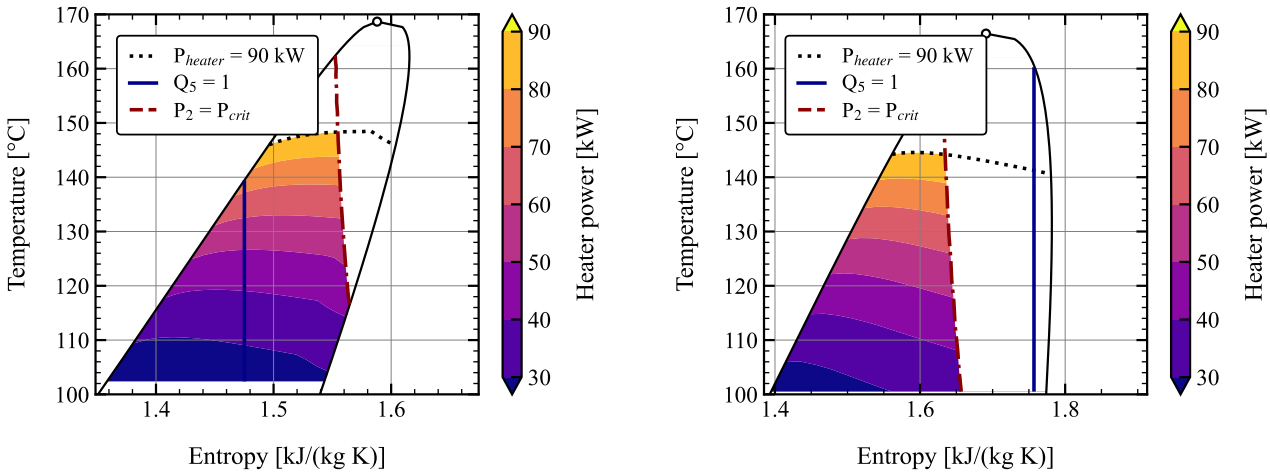

(a) Novec 649 heater power

(b) R1233zd(E) heater power

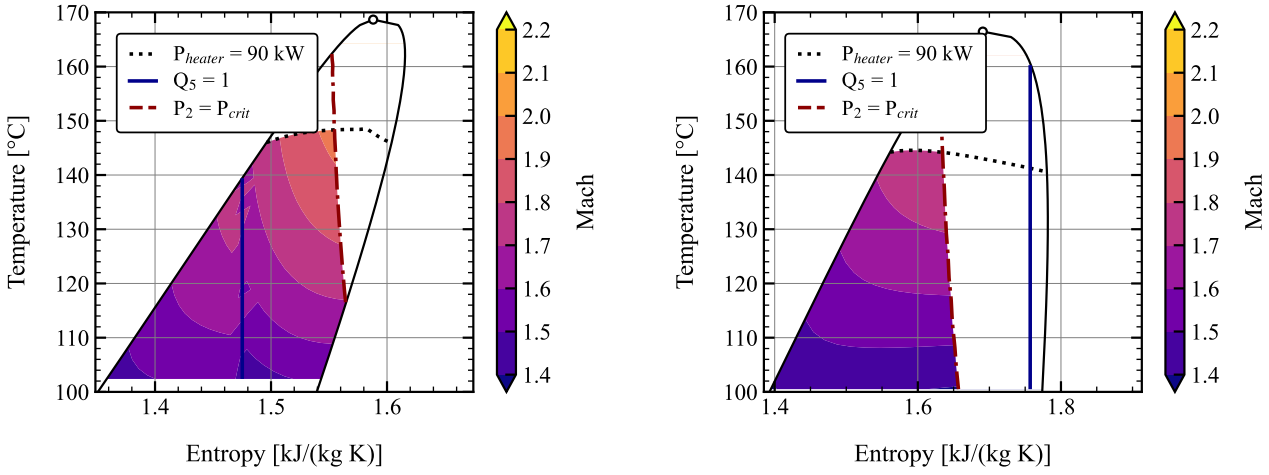

(c) Novec 649 Mach number

(d) R1233zd(E) Mach number

Figure 3: Parametric study of turbine inlet conditions, shown in temperature-entropy diagrams

4.2 Test rig operating envelope

A parametric analysis was conducted by varying the turbine inlet quality between 0.0 and 1.0, and the reduced inlet temperature between 0.85 and 0.99, while keeping the condensation temperature equal to 60 °C. Figure 3 presents the contour plots of heater power and nozzle Mach number as a function of turbine inlet conditions in the temperature-entropy diagram. The contour plot is limited by two lines: the dash-dotted one is the isenthalpic line where the fluid at the heater outlet reaches the critical pressure (after which point the definition of subcooling cannot be applied), while the dotted line represents the condition for which the maximum heater power is reached. It can be noticed that the heater power is relatively insensitive to inlet quality, because the increase in inlet enthalpy is balanced by a reduction in density, and correspondingly a reduction in choking mass flow rate. On the other hand, the power decreases significantly as temperature decreases, due to the combined effect of lower inlet enthalpy and density in the throat, which is mainly influenced by the density of the saturated vapor. The Mach number contours indicate that this quantity is highly sensitive to the inlet enthalpy, with the values increasing with quality at constant inlet temperature. Figure 3c shows a discontinuity in the Mach number where the turbine outlet reaches the saturated vapor, which is a consequence of the discontinuity in the local speed of sound across the vapor saturation line, rather than a discontinuity in the velocity. For both fluids the Mach number remains supersonic at all investigated conditions.

Based on the results of the parametric analysis, the following limiting conditions are considered as a guideline for the component sizing:

- The condenser should be sized at the high-temperature and high-quality corner of the operating envelope. For dry fluids such as Novec 649, this condition corresponds to the maximum amount of desuperheating that needs to be achieved in the condenser. Given the low heat transfer coefficient, this condition increases the minimum required area. For other fluids, such as R1233zd(E) where the turbine outlet is always two-phase, this condition still corresponds to the highest volumetric flow rate due to higher quality at the turbine outlet. Furthermore, the sizing can be done by re-computing the cycle solution with $\eta_{\text{is,t}} = 0$ to maximize the cooling duty.
- The heating circuit should be sized on the high-temperature and high-quality corner. In this point the temperature and pressure at the heater outlet are maximum, as well as the heater duty.
- The pump should be sized accounting for several conditions in the operating envelope: (i) the high-temperature and low-quality corner, where the mass flow rate is maximum; (ii) the high-temperature and high-quality corner, where the head is maximum; (iii) the low-temperature high-quality corner, where high head and low mass flow rate coexist, must be within the stable operating region of the pump, accounting for minimum flow requirements which are sometimes encountered in centrifugal pumps.
- The turbine aerodynamic design should target an intermediate point (e.g. $x_4 = 0.15$ and $T_{4r} = 0.9$), in such a way that both under- and over-expanded nozzle conditions can be reached. The maximum rotational speed should at least be equal to the highest optimal rotational speed within the envelope, which is expected to occur at the high-temperature, high-quality point due to the higher enthalpy difference.

5 Conclusions and future work

The deployment of two-phase turboexpanders holds significant potential for improving the thermodynamic efficiency of partial-evaporation organic Rankine cycles, heat pumps, and refrigeration systems. However, the commercialization and optimization of these machines have been hindered by a lack of high-fidelity experimental data and validated design guidelines. To bridge this gap, this paper detailed the comprehensive design of a 100 kW-thermal laboratory-scale test facility dedicated to the characterization of two-phase turboexpanders.

A primary challenge in two-phase experimental setups is the accurate determination of the thermodynamic state at the turbine inlet. To address this, an innovative measurement strategy utilizing an isenthalpic throttling valve was integrated into the system design, allowing for precise determination of the inlet vapor quality without the uncertainties associated with traditional energy-balance methods. Additionally, the test rig architecture includes a dedicated heat exchanger to ensure controllable and stable subcooling at the pump inlet, safeguarding the equipment against cavitation.

A rigorous fluid screening and thermodynamic scaling analysis identified Novec 649 as the most suitable working fluid for this laboratory-scale application. Despite its higher cost, Novec 649 provides an optimal balance of safety (non-flammable and non-toxic) and environmental sustainability (low GWP and zero ODP). Crucially, its low speed of sound and specific thermodynamic properties allow for a larger turbine throat area and a manageable rotational speed. Furthermore, as a dry fluid, Novec 649 enables the investigation of both two-phase and wet-to-dry expansion regimes within the same facility. A parametric analysis of the operating envelope further established the boundary conditions required for sizing the primary test rig components, ensuring robust operation across a wide range of turbine inlet qualities and temperatures.

Future work will focus on the construction, commissioning, and operation of the proposed test facility. The upcoming experimental campaigns will map the performance and efficiency of prototype two-phase turboexpanders across varying phase fractions and pressure ratios. Ultimately, the datasets generated by this facility will be used to validate multiphase computational fluid dynamics (CFD)

models, investigate non-equilibrium phase change phenomena, and establish reliable design and scaling guidelines for two-phase turbines.

Acknowledgments

The research presented in this paper has received funding from the European Union's research and innovation programme Horizon Europe grant agreement no. 101192974 (Project: EMPOWER). Disclaimer: Funded by the European Union. Views and opinions expressed are however those of the author(s) only and do not necessarily reflect those of the European Union or CINEA. Neither the European Union nor the granting authority can be held responsible for them.
Furthermore, the research was partly developed within the project "Sustainable large-scale energy storage in Egypt" (project no. 21-M13-DTU), funded by the Ministry of Foreign Affairs of Denmark and administered by the Danida Fellowship Center. The financial support is gratefully acknowledged.

References

[1] I. K. Smith, Development of the trilateral flash cycle system: Part 1: Fundamental considerations, Proceedings of the Institution of Mechanical Engineers 207 (3) (1993) 179–194. doi:10.1243/PIME_PROC_1993_207_032_02.

[2] C. Wieland, C. Schifflechner, K. Braimakis, F. Kaufmann, F. Dawo, S. Karellas, G. Besagni, C. N. Markides, Innovations for organic Rankine cycle power systems: Current trends and future perspectives, Applied Thermal Engineering 225 (2023) 120201. doi:10.1016/j.applthermaleng.2023.120201.

[3] D. M. Robinson, E. A. Groll, Efficiencies of transcritical CO_2 cycles with and without an expansion turbine, International Journal of Refrigeration 21 (7) (1998) 577–589. doi:10.1016/S0140-7007(98)00024-3.

[4] C. Tammone, R. Pili, S. Indrehus, F. Haglind, Techno-economic analysis of partial evaporation organic Rankine cycle systems for geothermal applications, in: Proceedings of the 6th International Seminar on ORC Power Systems, 2021, p. 10. doi:10.14459/2021mp1633026.

[5] H. K. Ersoy, N. Bilir, Performance characteristics of ejector expander transcritical CO2 refrigeration cycle, Proceedings of the Institution of Mechanical Engineers, Part A: Journal of Power and Energy 226 (5) (2012) 623–635. doi:10.1177/0957650912446547.

[6] M. Francesconi, S. Briola, M. Antonelli, A review on two-phase volumetric expanders and their applications, Applied Sciences 12 (20) (2022) 10328. doi:10.3390/app122010328.

[7] I. K. Smith, N. Stošič, C. A. Aldis, Development of the trilateral flash cycle system: Part 3: The design of high-efficiency two-phase screw expanders, Proceedings of the Institution of Mechanical Engineers, Part A: Journal of Power and Energy 210 (1) (1996) 75–93. doi:10.1243/PIME_PROC_1996_210_010_02.

[8] F. Dawo, J. Buhr, C. Wieland, H. Spliethoff, Experimental investigation of the partially evaporated organic rankine cycle for various heat source conditions, in: Proceedings of the 6th International Seminar on ORC Power Systems, 2021, pp. 1–9. doi:10.14459/2021mp1633102.

[9] F. Dawo, J. Buhr, C. Schifflechner, C. Wieland, H. Spliethoff, Experimental assessment of an Organic Rankine Cycle with a partially evaporated working fluid, Applied Thermal Engineering 221 (2023) 119858. doi:10.1016/j.applthermaleng.2022.119858.

[10] M. Youbi-Idrissi, J. Bonjour, The effect of oil in refrigeration: Current research issues and critical review of thermodynamic aspects, International Journal of Refrigeration 31 (2) (2008) 165–179. doi:10.1016/j.ijrefrig.2007.09.006.

[11] G. Zywica, T. Z. Kaczmarczyk, E. Ihnatowicz, A review of expanders for power generation in small-scale organic Rankine cycle systems: Performance and operational aspects, Proceedings

of the Institution of Mechanical Engineers, Part A: Journal of Power and Energy 230 (7) (2016) 669–684. doi:10.1177/0957650916661465.

[12] E. Bellos, A review of organic Rankine cycles with partial evaporation and dual-phase expansion, Sustainable Energy Technologies and Assessments 72 (2024) 104059. doi:10.1016/j.seta.2024.104059.

[13] R. I. Crane, Droplet deposition in steam turbines, Proceedings of the Institution of Mechanical Engineers, Part C: Journal of Mechanical Engineering Science 218 (8) (2004) 859–870. doi:10.1243/0954406041474200.

[14] P. Welch, P. Boyle, New turbines to enable efficient geothermal power plants, Geothermal Resources Council Transactions 33 (2009) 765–772.
URL https://publications.mygeoenergynow.org/grc/1028557.pdf

[15] L. G. Hays, A. Otsuka, P. Boyle, Sea trials of an organic triangle system (OTC) for waste heat recovery, in: Proceedings of the 6th International Seminar on ORC Power Systems, 2021, p. 145. doi:10.14459/2021mp1633147.

[16] A. Kumar, S. Parisi, R. Agromayor, J. H. Walther, F. Haglind, Unsteady computational fluid dynamics analysis of end-sector losses in a two-phase axial turbine with partial admission, Journal of Engineering for Gas Turbines and Power 148 (061022) (2026). doi:10.1115/1.4070567.

[17] G. Lhermet, N. Tauveron, N. Caney, Q. Blondel, F. Morin, A recent advance on partial evaporating organic rankine cycle: Experimental results on an axial turbine, Energies 15 (20) (2022). doi:10.3390/en15207559.

[18] S. Quoilin, M. V. D. Broek, S. Declaye, P. Dewallef, V. Lemort, Techno-economic survey of organic rankine cycle (orc) systems, Renewable and Sustainable Energy Reviews 22 (2013) 168–186. doi:10.1016/j.rser.2013.01.028.

[19] A. Manera, B. Ozar, S. Paranjape, M. Ishii, H.-M. Prasser, Comparison between wire-mesh sensors and conductive needle-probes for measurements of two-phase flow parameters, Nuclear Engineering and Design 239 (9) (2009) 1718–1724. doi:10.1016/j.nucengdes.2008.06.015.

[20] I. H. Bell, J. Wronski, S. Quoilin, V. Lemort, Pure and pseudo-pure fluid thermophysical property evaluation and the open-source thermophysical property library coolprop, Industrial & Engineering Chemistry Research 53 (6) (2014) 2498–2508. doi:10.1021/ie4033999.

[21] E. W. Lemmon, I. H. Bell, M. L. Huber, M. O. McLinden, NIST Standard Reference Database 23: Reference Fluid Thermodynamic and Transport Properties-REFPROP, Version 10.0, National Institute of Standards and Technology (2018). doi:10.18434/T4/1502528.

[22] S. L. Dixon, C. A. Hall, Fluid Mechanics and Thermodynamics of Turbomachinery, Elsevier, 2014. doi:10.1016/C2011-0-05059-7.

[23] H. Schlichting, K. Gersten, Boundary-Layer Theory, Springer Berlin Heidelberg, 2017. doi:10.1007/978-3-662-52919-5.

[24] M. Pilch, C. Erdman, Use of breakup time data and velocity history data to predict the maximum size of stable fragments for acceleration-induced breakup of a liquid drop, International Journal of Multiphase Flow 13 (6) (1987) 741–757. doi:10.1016/0301-9322(87)90063-2.

[25] A. Cioffi, S. Parisi, R. Agromayor, F. Haglind, Extension of the method of characteristics for the design of supersonic stators in two-phase turbines, in: Proceedings of the Turbo Expo 2026 (Accepted), 2026.